Bakker A., Van den Akker H.E.A. (1990) The Use of Profiled Axial Flow Impellers in Gas-Liquid Reactors. Fluid Mixing IV, IChemE, 11-13 September 1990, Bradford, U.K., symposium series 121, page 153-166.

THE USE OF PROFILED AXIAL FLOW IMPELLERS IN GAS-LIQUID REACTORS

A. Bakker and H.E.A. van den Akker*

In recent years a variety of profiled axial flow impellers has been developed. The aim of the present research work is to investigate the performance of these impellers and to contribute to the understanding of the gas dispersion mechanism. Three impeller types have been compared: a standard inclined blade impeller and the profiled A315 and Leeuwrik impeller. Important parameters are pumping capacity, turbulence intensity, gas dispersion performance, power consumption and mass transfer. It is concluded that in most of these respects the profiled impellers offer advantages over traditional impellers.

INTRODUCTION

Gas-liquid stirred vessels are often equipped with simple impellers which are cheap to make, like disc turbines or inclined blade impellers. Because of the industrial importance a lot of research has been done to describe the hydrodynamic properties of these impellers, see for instance Warmoeskerken et al. (1, 2), Chapman et al. (3) and Nienow et al. (4).

However, during the last few years several axially pumping, hydrodynamically profiled impellers have become available on the market. Examples of such impellers are the Lightnin A310 and A315, the Ekato Intermig and Interprop and the Prochem hydrofoil. In general, the manufacturers claim that at a given level of power input these impellers are capable of dispersing more gas and yield higher mass transfer coefficients than conventional impellers. For example, it is reported that mass transfer could be enhanced by up to 30% on average by replacing a disc turbine by a Lightnin A315 system (Oldshue (5)).

The aim of the present research work is to investigate the performance of a number of profiled impellers and to contribute to the understanding of the gas dispersion mechanism when such impellers are used. Therefore various impellers are compared on the basis of pumping efficiency, turbulence intensity, power consumption, gas handling capacity and mass transfer performance. Impellers used are a Lightnin A315, the Dutch Leeuwrik impeller and a traditional inclined flat blade turbine.

* Kramers Laboratorium voor Fysische Technologie, Delft University of Technology, Prins Bernhardlaan 6, 2628 BW, Delft, The Netherlands

THEORETICAL BACKGROUNDS

The spatial distribution of the gas bubbles in a stirred vessel is largely determined by the overall flow pattern and the strength of the liquid flow. Two classes of gas-liquid dispersions can be distinguished.

In the first class a disk turbine is used as impeller. The gas issuing from the sparger rises into the impeller and is dispersed from there. It has been shown that the turbulence induced in the vessel is extremely non uniform with very high dissipation levels in the immediate vicinity of the impeller and very much lower levels elsewhere (Laufhütte and Mersmann (6)). Therefore the spatial bubble size distribution is also non-uniform. Bubble break-up occurs mainly in the impeller outflow. The resulting bubbles are small. Due to coalescence much larger bubble sizes are found in the liquid bulk (Greaves and Barigou (7)).

The second class of stirred dispersions is obtained by using a downwards pumping impeller. As the rising gas-flow is counteracted by the downward liquid flow, the gas does not enter the impeller directly but is distributed over the contents of the vessel by the strong circulatory flow. Only part of the gas is recirculated and redispersed by the impeller. As a consequence bubble size may, apart from the initial size, to a large extent depend on processes of breakup and coalescence in the liquid bulk. Therefore, turbulence intensity should be distributed as uniformly as possible. At high gassing rates, however, the downward liquid flow will not be sufficient to overcome and deflect the rising gas flow. The gas will rise directly into the impeller and the homogeneity of the dispersion becomes worse. This so-called indirect loading to direct loading transition has been described by (2). It will be clear that it is essential to postpone this transition as long as possible. The strong liquid flow which is required to do so, renders pumping efficiency an important parameter.

Defining the pumping efficiency

The pumping efficiency η can be defined as the ratio of the gain in enthalpy of the fluid, $\Delta p.Q_l$, to the power input P by the impeller. The pressure rise Δp over the impeller as determined by, among other things, rotational speed N and impeller geometry is converted into velocity head of a circulatory flow:

$$\Delta p = K_w \frac{1}{2} \rho_l \bar{v}^2 \sim \rho_l Q_l^2/T^4 \qquad (1)$$

The proportionality constant K_w depends on the vessel geometry only and is not known in general. Now, by using the dimensionless power number Po and the pumping number N_q:

$$Po = P/(\rho_l N^3 D^5); \qquad N_q = Q_l/(N D^3); \qquad (2)$$

the following relation can be found:

$$\eta = \Delta p\, Q_l/P \sim (D/T)^4 N_q^3/Po \qquad (3)$$

Since the absolute value of η can not be calculated from eq. (3), the impellers will be compared on basis of the pumping efficiency relative to the inclined blade impeller ($45^{\downarrow}6$): $\eta' = \eta/\eta(45^{\downarrow}6)$

The impellers used

Three impellers are compared during the present research: a Lightnin A315, the Dutch Leeuwrik impeller and a traditional inclined flat blade turbine.

Gas-liquid dispersion using downwards pumping impellers with flat inclined blades has been discussed by several authors. The influence of sparger geometry and impeller position in two-phase and three-phase systems has been investigated (3, 4). Mass transfer and power consumption proved to be strongly related to the process of cavity formation (2). Furthermore, it has been reported that with respect to mass transfer efficiency an inclined blade impeller performs at least as well as a Rushton turbine (2).

The design of the Leeuwrik impeller was carried out by the Netherlands Organization for Applied Scientific Research TNO (Vermeulen and Pohlmann (8)). This impeller is meant to create a large liquid flow as well as a strong trailing vortex. The large flow should increase the homogeneity of the dispersion whereas the vortex should decrease the size of the recirculated bubbles. The plan form of the blades is based on the shape of a delta wing. Wings of this type yield a large lift and produce strong trailing vortices (fig. 1a). These delta wings can be mounted on a hub (fig. 1b). Profiling the blades and adjusting the pitch gives the shape of the Leeuwrik impeller (fig. 1c). Van den Akker and Bakker (9) visualized the trailing vortex by means of cavitation techniques, see fig. 2.

The A315 is a relatively new impeller design, commercially available from Mixing Equipment Co (Rochester U.S.A.). This four-bladed impeller is characterized by the large blades and rounded edges (figure 3). According to Oldshue et al. (5, 10) this impeller is capable of dispersing 86% more air than a disc turbine at the same power input. At the same power input, gassing rate and torque, but different D/T ratio, it was found that gas-liquid mass transfer could be enhanced by 30% on average by using an A315 system instead of a conventional disc turbine system.

EXPERIMENTAL

The experimental equipment is shown in figure 4. First, a vessel was used for laser-doppler measurements of velocities in a liquid-only mode of operation. This vessel was provided with a draft tube being 0.19m in diameter. The liquid level above the draft tube was 0.20m. Laser-doppler measurements were made at 0.20m and 0.60m below the impeller. The pumping capacities of the impellers were obtained from the measured velocity profiles.

Second, a flat-bottomed vessel of diameter T=0.44m was used for the gas dispersion experiments. The vessel was equipped with four baffles (width W=0.1T). The liquid height H was equal to the tank diameter T throughout the experiments. A ring sparger of diameter d_s=0.076m, provided with 31 holes and mounted at a separation distance of S=0.7D was used for most gas-liquid experiments. An additional separation distance S=0.3D was tested with the A315. Impeller-bottom clearance equalled C=0.4T in most cases.

Mass transfer experiments were done using a conventional dynamic method. The mass transfer coefficient $k_l a$ was calculated from the increase in oxygen concentration after a step change of inlet gas from nitrogen to air. Distilled water was used as continuous phase during these experiments.

In both vessels power demand was calculated from the impeller rotational speed and the torque on the shaft. The torque was determined with a Vibro-torque transducer mounted in the shaft. Impeller dimensions can be found in table 1.

SINGLE-PHASE FLOW

The draft-tube vessel was used for measuring the pumping capacity of the various impellers. The average velocity ($\bar{v}_{ax}$) and the fluctuating component (v'_{ax}=RMS($v_{ax}-\bar{v}_{ax}$)) of the axial velocity have been measured at different radial distances in the draft tube at an impeller speed N=10Hz and at a distance of 0.20m below the impellers. The results for the three different impellers have been plotted in figure 5a,b. Figure 5c shows the relative turbulence intensity $v'_{ax}/\bar{v}_{ax}$.

The outflow of the Leeuwrik impeller (LS6) is dominated by the trailing vortex. The average velocity profile is rather flat near the centre of the draft-tube but shows a steep increase near the blade tip. The vortex also causes a high turbulence intensity. The velocity profiles of the 45↓6 and the A315 look rather different when compared with that of the LS6. With these impellers the average velocity profile flattens near the blade tip. The differences in shape of the turbulence profiles are remarkable. The turbulence intensity is constant near the centre for the LS6 but increases near the blade tip. For the 45↓6 and the A315 the turbulence intensity first decreases and only shows a weak increase towards the tip. On the average, the relative turbulence intensity is lowest for the A315. This will lead to lower shear stresses, which can be an advantage in shear-sensitive fermentation broths.

The results for the pumping efficiency are given in table 1. The A315 clearly has the highest pumping efficiency. These results qualitatively agree with the findings of Weetman and Oldshue (11). In fact, they find a smaller difference between the A315 and the 45↓6 but this is possibly due to a difference in vessel geometry and especially the fact that radial flow is suppressed in the draft tube. It is also possible that the larger diameter of the A315 is advantageous in draft-tube systems. The LS6 does have a larger efficiency than the 45↓6 but the difference is rather small compared to the difference with the A315. Probably the LS6 loses too much energy in the vortex near the blade tip: a substantial part of the power supplied to the impeller is directly converted into turbulent kinetic energy rather than into velocity head of a mean circulatory flow. The high value of Po of the LS6 is striking too.

GAS-LIQUID DISPERSION

Power consumption

The 0.44m standard vessel was used for two-phase experiments. Power consumption and mass-transfer coefficients were measured as a function of gassing rate and impeller speed for the different impellers.

TABLE 1 - Impeller diameter, power number, pumping capacity and pumping effficiency in the two vessels

Impeller	Draft tube vessel				Standard vessel	
	D(m)	Po	N_q	η'	D(m)	Po
45↓6	0.167	1.27	0.66	1.00	0.176	1.75
LS6	0.168	2.55	0.93	1.42	0.168	2.48
A315	0.178	0.76	0.66	2.12	0.178	0.76

The increase in radial flow produced by the 45↓6 when placed in the standard vessel, which is suppressed in the draft-tube, leads to an increase of almost 40% in the power number (table 1). The power numbers of the LS6 and the A315 do not differ significantly in the draft tube and the standard vessel, which means that these impellers maintain a strong axial flow.

The gassed power curves from the LS6 and the 45↓6 have been plotted in fig. 6b. The ratio between gassed and ungassed power consumption is denoted by P_g/P_u and Fl denotes the gas-flow number.

When using a LS6 the gassed power shows a steep increase at low impeller speeds. It was determined visually that this increase coincides with a transition from indirect loading and good dispersion to direct loading and bad gas dispersion. At the same time, the flow pattern switches from axial flow to radial flow. This transition in flow pattern leads to a sharp increase in power number. The gas-flow number at which this transition occurs increases with impeller speed. At high impeller speeds (N>6Hz) such a flow transition was not observed, in the investigated gassing range.

The power curves from the 45↓6 agree well with those obtained by (2). The lower value of P_g/P_u at Fl>0.05 for N=6Hz compared to N=4Hz is caused by the larger cavity size at higher impeller speeds.

Two sparger positions have been tested for the A315: S=0.3D and S=0.7D. The power curves for these two positions are plotted in figure 7. The power drop in the curves coincides with an indirect-direct loading transition. This occurs earlier for the smaller separation distance. Therefore, it can be concluded that a large separation distance is beneficial.

For this large separation distance the power curves have been studied more closely (fig. 8). At low impeller speeds the power consumption increases with gassing rate. This agrees fairly well with the findings of Lally (12). The flow pattern near the impeller has been studied photographically. It is found that the process of cavity formation is analogous to that for inclined blade impellers. At low gassing rates, Fl<0.01, vortex cavities are formed. At increasing gassing rates the cavity size increases and growing cavities are formed. This coincides with the increase in P_g/P_u at low speeds (N=4Hz and N=5Hz). At still higher gassing rates (Fl≈0.04, depending on impeller speed) large cavities are formed, power consumption decreases and gas dispersion becomes worse. Consequently, in order to achieve good gas dispersion this impeller should be operated in the vortex/growing cavity regime.

In general the A315 is capable of dispersing more air than the 45↓6. For example at an impeller speed of N=6Hz the indirect loading to direct loading transition occurs at Fl≈0.045 for the A315 and at Fl≈0.03 for the 45↓6. Because of the lower power number of the A315 power consumption is also lower.

Mass transfer

The mass-transfer coefficient was determined as a function of gas flow rate and impeller speed for all three impeller types. Figure 6a shows the results for the LS6 and the 45↓6. Figure 9 shows the results for the A315.

Study of the mass transfer curves for the 45↓6 makes clear that stirrer hydrodynamics does not only influence the power curves but, as a consequence, also effects mass transfer. The dips in the curves correspond to the drop in power consumption at the formation of large cavities. The opposite is not

always true: for the LS6 the increase in power consumption at the axial-radial flow transition at N=4Hz does not lead to an increase in $k_l a$. Here the larger power dissipation does not lead to a better gas-dispersion. The mass transfer curves for the A315 are in general flatter and do not show such dips.

Figure 10 shows $k_l a$ as a function of specific power consumption at constant superficial gas velocity (v_{sg} = 0.01 m/s). Both the A315 and the LS6 yield a mass transfer coefficient which is larger than when using the 45↓6. An explanation could be that the larger pumping efficiency of the A315 and the LS6 results in a larger gas-holdup and hence in a larger mass transfer. When compared at equal impeller-bottom clearance (C/T=0.4) the difference between the A315 and the LS6 is only small. For the A315 $k_l a$ increases when clearance is decreased to C/T=0.3, possibly due to an increase in gas holdup. Because of it's stability and good mass transfer performance it seems advantageous to use an A315 rather than a 45↓6 or a LS6.

Some remarks with respect to interpreting this result should be made. Firstly, the geometries used are not optimal. Mixing Equipment Co. advises to use a larger ring sparger for the A315. Secondly, our comparison is made for impellers at equal D/T ratio. The D/T ratio is important when retrofitting existing installations. In such a case impeller speed, power consumption and torque are given parameters. This imposes restrictions on the D/T ratio of the new impeller. A comparison at different D/T ratios might give slightly different results.

CONCLUSIONS

Several aspects of the behaviour of three axial flow impellers have been studied. It may be concluded that modern, profiled impellers like the A315 and the Leeuwrik impeller can offer advantages over traditional inclined blade impellers. The A315 gave the best overall performance from the impellers tested.

The profiled A315 and Leeuwrik impeller do have larger pumping efficiencies than the inclined blade impeller. This can lead to a better gas dispersion and higher mass transfer coefficients. The A315 creates lower turbulence intensities and shear stresses than the other two impellers, which can be advantageous in shear sensitive fermentation broths.

It is expected that impeller performance can be improved by optimizing the reactor geometry. However, the influence of liquid properties and geometrical parameters like impeller-bottom clearance, D/T ratio and sparger has not yet been studied. Further research in this area is useful.

For a better understanding of the processes which occur in the vessel detailed knowledge of the internal structure of the gas-liquid dispersion is necessary. This will be the subject of future study.

These investigations are supported by the Netherlands Technology Foundation (STW, DTN 44.0566). The A315 impeller was kindly put at our disposal by Mixing Equipment Co.

NOMENCLATURE

C = impeller-bottom clearance (m)

d_s = sparger diameter (m)

D = impeller diameter(m)

Fl = gas flow number (-)

k_la = mass transfer coefficient (s^{-1})

K_w = friction coefficient (-)

N_q = pumping number (-)

Q_g = gas flow (m^3s^{-1})

Q_l = liquid flow through the draft tube (m^3s^{-1})

P = power consumption (W)

Po = impeller power number (-)

S = impeller-sparger separation (m)

T = vessel diameter (m)

v_{sg} = superficial gas velocity (ms^{-1})

$\bar{v}_{ax}$ = local mean axial liquid velocity (ms^{-1})

v'_{ax} = local velocity fluctuation (ms^{-1})

$\bar{v}$ = average axial liquid velocity in the draft tube vessel (ms^{-1})

Δp = pressure rise at impeller (Pa)

η = pumping efficiency (-)

ρ_l = liquid density (kgm^{-3})

REFERENCES

1. Warmoeskerken M.M.C.G., Smith J.M., 1982, Proceedings 4th Eur.Conf.Mixing, BHRA Fluid Engineering, Cranfield U.K., 237-246

2. Warmoeskerken M.M.C.G., Speur J., Smith J.M., 1984, Chem.Eng.Com. 25 11-29

3. Chapman C.M., Nienow A.W., Cooke M., Middleton J.C., 1983, Chem.Eng.Res.Des. 61, 71-95 and 167-185

4. Nienow A.W., Konno M., Bujalski W., 1986, Chem.Eng.Res.Des. 64, 35-42

5. Oldshue J.Y., 1989, Chemical Engineering Progress 5, 33-42

6. Laufhütte H.D., Mersmann A.B., 1985, Proceedings 5th. Eur.Conf.Mixing, BHRA Fluid Engineering, Cranfield U.K., 331-340

7. Greaves M., Barigou M., 1988, Proceedings 6th Eur.Conf.Mixing, BHRA Fluid Engineering, Cranfield U.K., 313-320

8. Vermeulen P.E.J., Pohlmann J.W., 1980, "Ontwikkeling van de Leeuwrikschroef", Internal report MT-TNO, Ref.nr. 80-015586, (Dutch)

9. Van den Akker H.E.A., Bakker A., 1989, MIXING XII, Trout Lodge U.S.A.

10. Oldshue J.Y., Post T.A., Weetman R.J., Coyle C.K., 1988, Proceedings 6th Eur.Conf.Mixing, BHRA Fluid Engineering, Cranfield U.K., 345-350

11. Weetman R.J., Oldshue J.Y., 1988, Proceedings 6th Eur.Conf.Mixing, BHRA Fluid Engineering, Cranfield U.K., 43-50

12. Lally K.S., 1987, Mixing Equipment Technical Report #A315-2

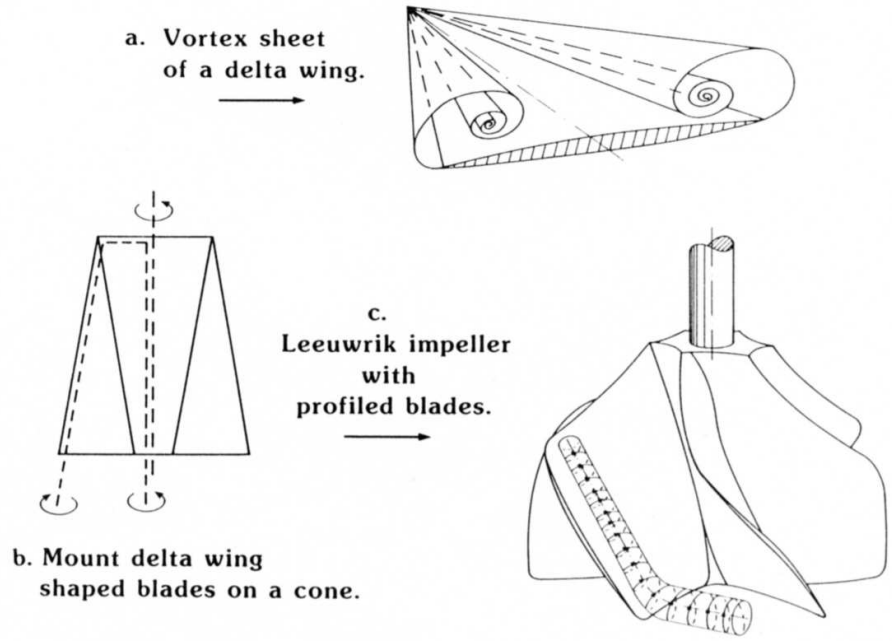

Figure 1 a,b,c The design of the Leeuwrik impeller.

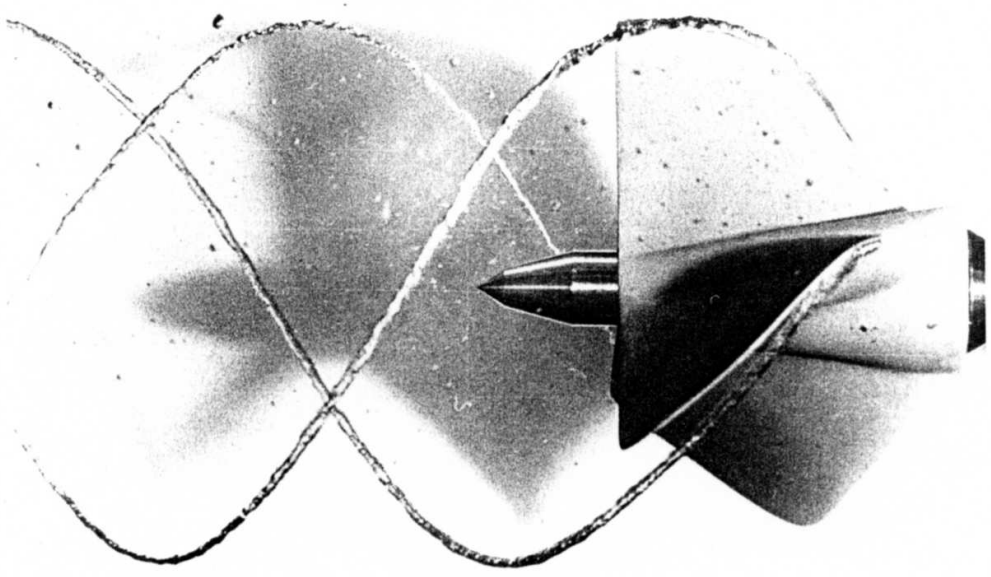

Figure 2 The trailing vortex behind the blade of a three-bladed Leeuwrik impeller as visualized in a cavitation tunnel. The vortex is filled with vapour.

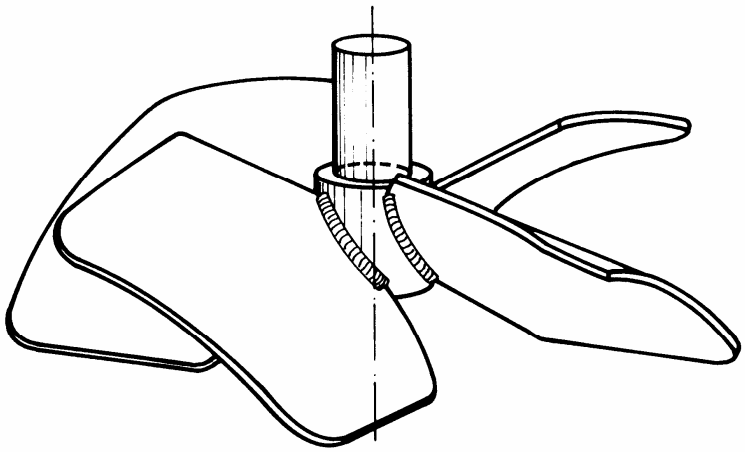

Figure 3 The A315 impeller.

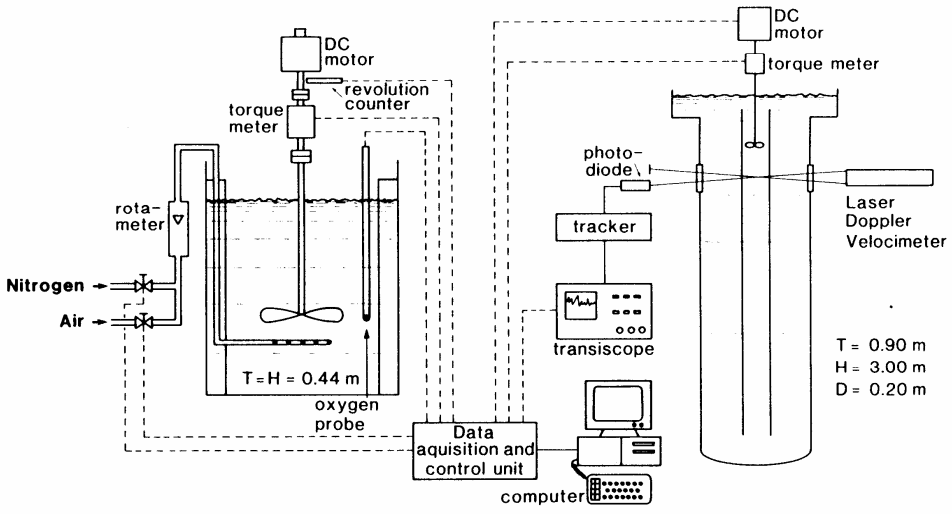

Figure 4 The experimental equipment.

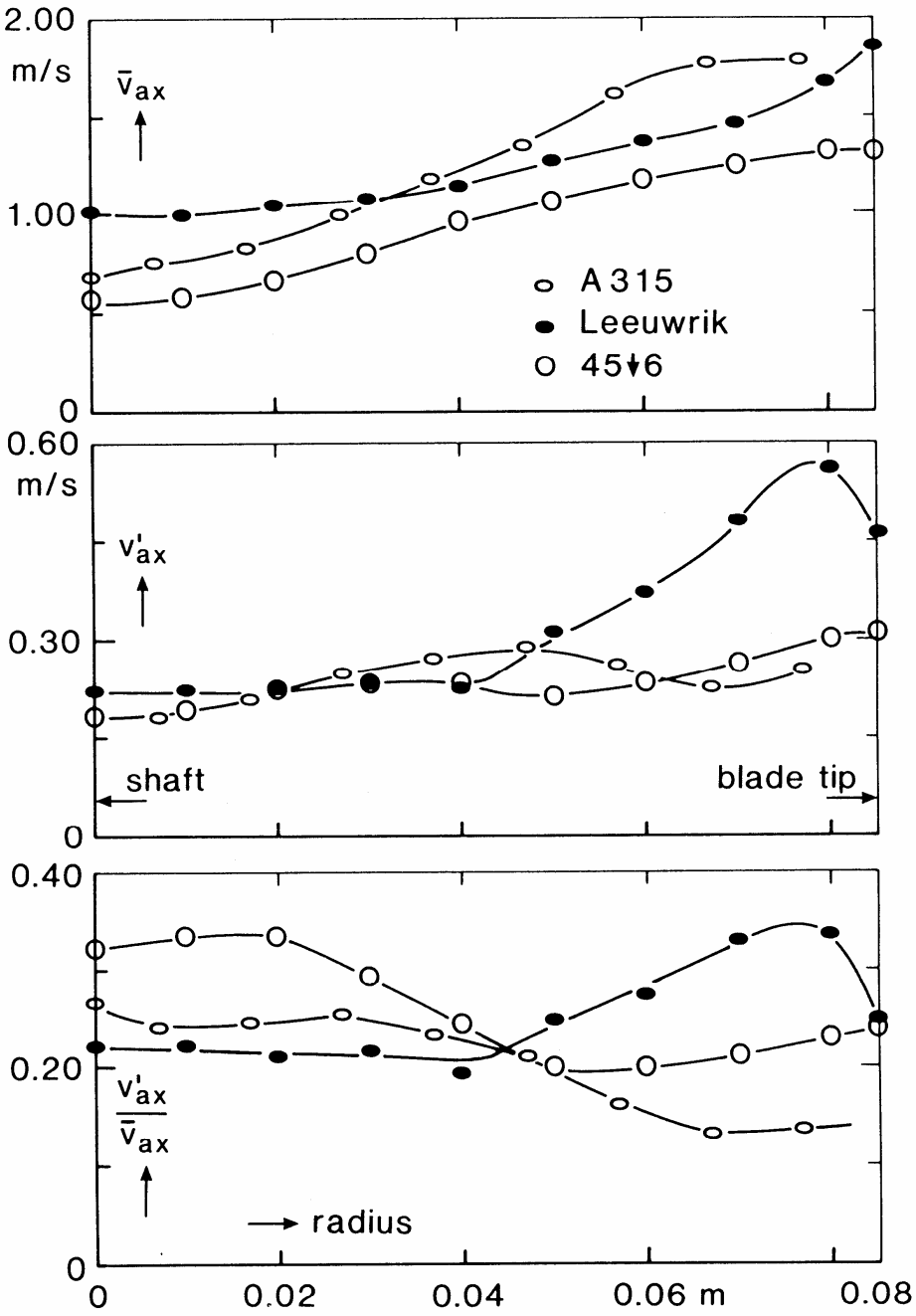

Figure 5 a,b,c Axial velocity and turbulence intensity below the impellers as measured in the draft-tube vessel.

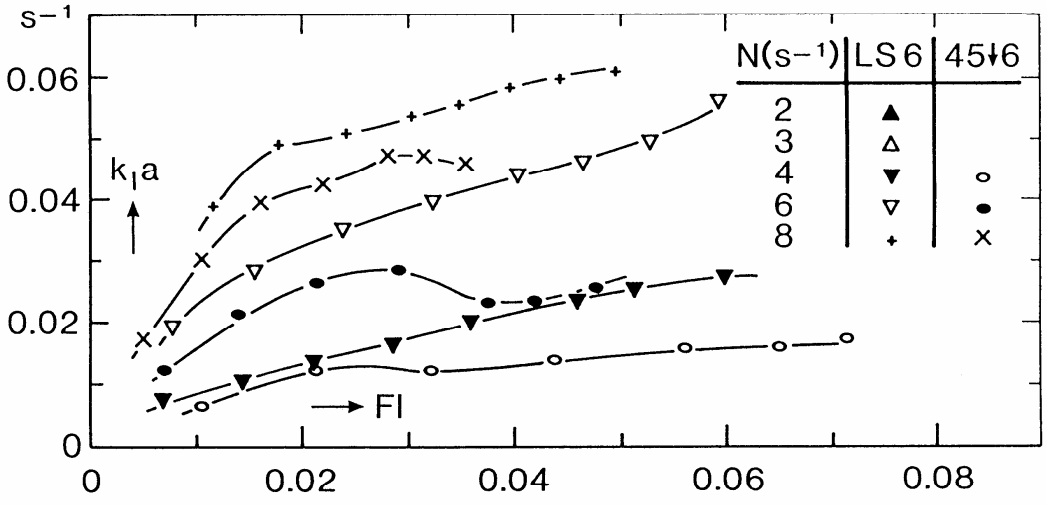

Figure 6a Mass transfer as a function of Fl and N for both the Leeuwrik impeller (LS6) and the inclined blade impeller.

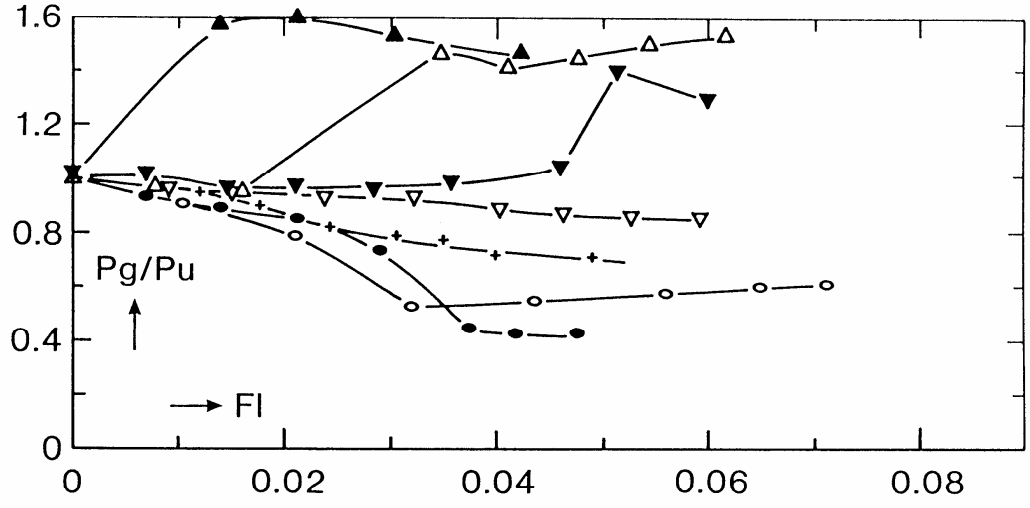

Figure 6b P_g/P_u as a function of Fl and N. Legend as in figure 6a.

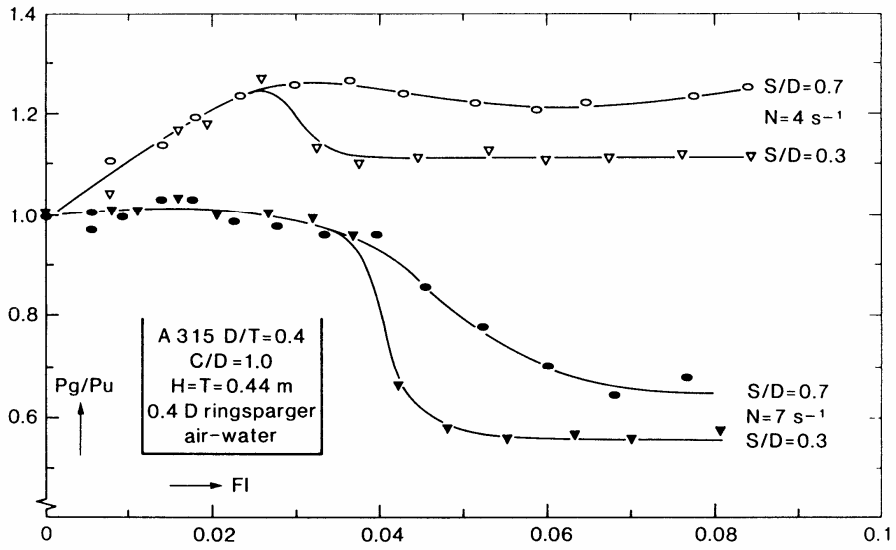

Figure 7 The power curves for the A315 impeller at two different impeller-sparger separation distances.

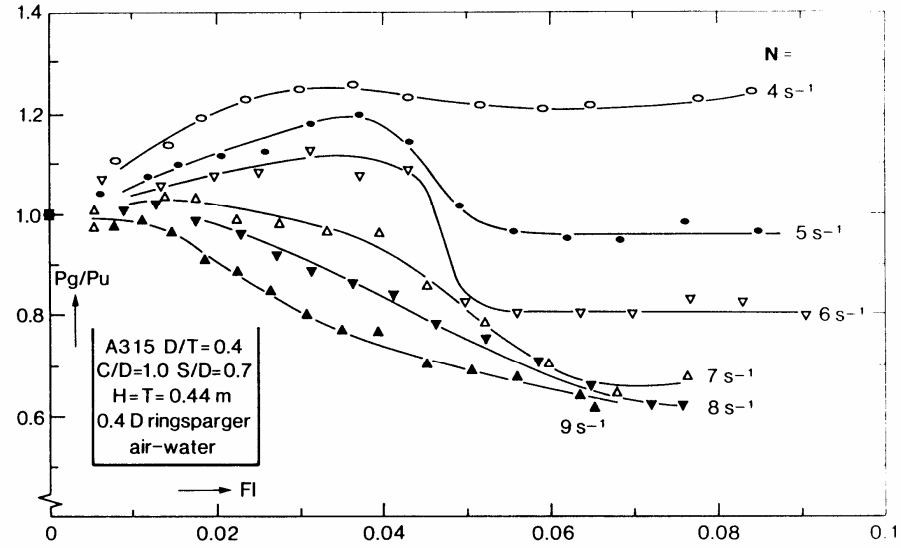

Figure 8 The power curves for the A315 impeller at the large impeller sparger separation distance.

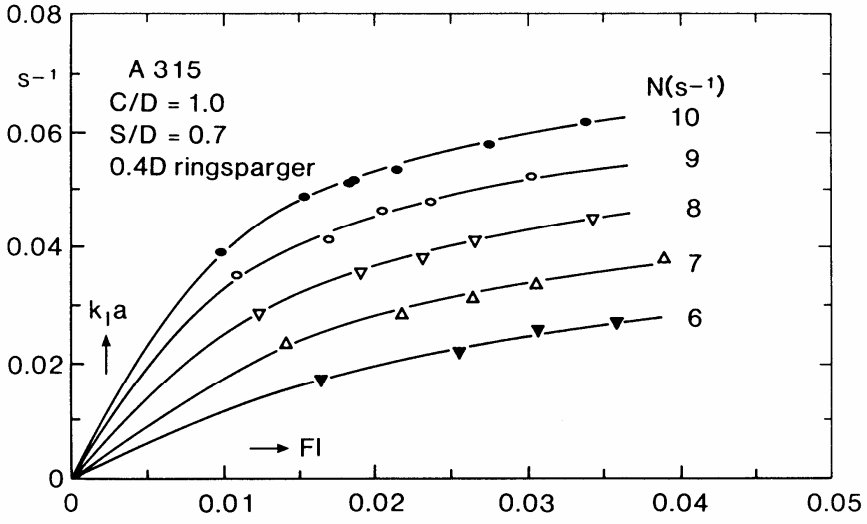

Figure 9 K_la as a function of gas-flow number and impeller speed for the A315 impeller.

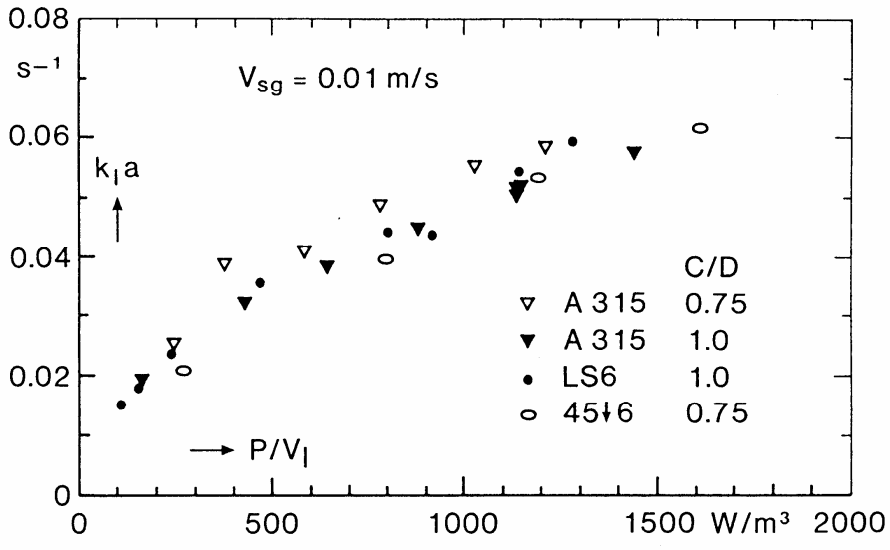

Figure 10 The mass transfer coefficient as a function of power consumption at a superficial gas velocity v_{sg}=0.01 m/s.